DALTON
FULL PAPER

A new polymorph of $LiZnPO_4 \cdot H_2O$; synthesis, crystal structure and thermal transformation †

Torben R. Jensen*

Chemistry Department, University of Odense, DK-5230 Odense M, Denmark

A new polymorph of lithium zinc phosphate hydrate, β-$LiZnPO_4 \cdot H_2O$, has been obtained by hydrothermal synthesis, and its crystal structure and thermal transformation investigated. The crystal structure can be viewed as a framework structure built from PO_4 and ZnO_4 tetrahedra with LiO_4 tetrahedra and water molecules placed in eight-ring channels; β-$LiZnPO_4 \cdot H_2O$ is apparently the only member of the zeolite ABW group of materials crystallising in space group $P2_1ab$. It has a doubled *b* axis compared to a known phase of $LiZnPO_4 \cdot H_2O$. The ^{31}P MAS NMR spectrum showed two signals; δ 6.94(2) and 7.88(2). The known phase of $LiZnPO_4 \cdot H_2O$ transforms into β-$LiZnPO_4 \cdot H_2O$ after treatment in 0.9 M $LiNO_3$ (aq) at 80 °C and 10 kbar for 20 h. A mechanism for the pressure-induced displacive phase transition is proposed. Dry or hydrothermal heating of β-$LiZnPO_4 \cdot H_2O$ at >100 °C gave δ_1-$LiZnPO_4$. The enthalpy change for the dehydration with a maximum at 219(2) °C was determined to be $\Delta H = 43(6)$ kJ mol^{-1}, using differential scanning calorimetry.

Microporous materials have found extensive industrial use over the last decades, *e.g.* as gas absorbers, ion exchangers, catalysts and many other applications.[1] Such materials with new framework structures and compositions are of great importance as their function is often correlated with the internal shape and size of cages and channels and the position of metal ions in the material. Among new materials a large number of phosphates and some arsenates have been characterised during the last decade.[2]

The chemistry of zinc orthophosphates shows a large variety of phases mainly due to the co-ordination flexibility of the zinc ions and their ability to form Zn–O–Zn linkages.[3] An increasing number of orthophosphates are found in the system, ZnO–P_2O_5–cation, prepared by hydrothermal synthesis from aqueous or non-aqueous solutions using alkali-metal ions and/or organic amine ions as templates. There are several members of this group which are structural analogues to aluminosilicates, *e.g.* sodalite, zeolite-X and ABW,[4] but also compounds with novel crystal structures with no naturally occurring mineral counter part, *e.g.* $Zn_2(HPO_4)_3 \cdot H_3NCH_2CH_2NH_3$.[5] A member of this family, $Zn(H_2PO_4)(HPO_4) \cdot (CH_3)_4N$, possesses very low framework density, 10.1 tetrahedral framework atoms (T) per 1000 Å^3.[6] In general microporous materials are metastable as they transform to more dense phases upon heating either dry or hydrothermal. Careful adjustment of synthesis conditions is crucial for preparation of new materials, *e.g.* stabilisation and isolation of intermediate phases in the synthesis of more dense phases.

Hydrothermal preparation techniques have revealed the existence of several new lithium zinc phosphates and the crystallisation fields of the compounds are under further investigation.[7] A polymorph of $LiZnPO_4$ having a phenacite type structure (denoted ε-$LiZnPO_4$ in this work for distinction from the other polymorphs),[8] a cristobalite related phase, δ_1-$LiZnPO_4$,[9] and a polymorph (denoted α′-$LiZnPO_4$)[7] with a more complex crystal structure can all be prepared by hydrothermal methods. The compound α′-$LiZnPO_4$ is possibly structurally related to α-$LiZnPO_4$,[7] which is the stable phase under ambient conditions prepared by solid state reaction. A common feature of the lithium zinc phosphates, α-, ε- and δ_1-$LiZnPO_4$ (and possibly also α′-$LiZnPO_4$), are three-dimensional framework structures built from LiO_4, ZnO_4 and PO_4 tetrahedra forming six-ring channels.[7–10] The system Li_3PO_4–$Zn_3(PO_4)_2$ was studied by means of solid state reactions and thermal analysis. The equilibrium phase diagram shows the existence of four lithium zinc phosphates with the compositions $Li_4Zn(PO_4)_2$, $Li_9Zn_6(PO_4)_7$, $LiZnPO_4$ and '$LiZn_9(PO_4)_7$', and each of them may exist in one, two or three modifications. The phase diagram reveals that α-$LiZnPO_4$ transforms to β-$LiZnPO_4$ at 737 °C, γ-$LiZnPO_4$ at 1006 °C and melts at 1172 °C.[11] It is not possible to quench β- or γ-$LiZnPO_4$ to ambient conditions as the phase transitions are reversible and the only available structural data is a powder pattern of β-$LiZnPO_4$.[9b] A polymorph of $Li_4Zn(PO_4)_2$ and the mentioned phases of $LiZnPO_4$ seem to be the only compositions from the phase diagram that can be prepared by means of hydrothermal synthesis.[12]

A water-containing lithium zinc phosphate, $LiZnPO_4 \cdot H_2O$, was described having a zeolite type ABW structure, *i.e.* isomorphous with zeolite Li-A(BW), $LiAlSiO_4 \cdot H_2O$.[9a] An accurate structure analysis of $LiAlSiO_4 \cdot H_2O$ was performed by combining single crystal and powder diffraction data, using X-rays and neutron radiation, respectively.[13] The structure can be viewed as a framework built from AlO_4 and SiO_4 tetrahedra giving four- and eight-ring channels in the crystallographic *c* direction and six-ring channels in a perpendicular direction. The lithium ions are co-ordinated to three framework oxygen atoms and one water oxygen atom.[13]

The polymorph of $LiZnPO_4 \cdot H_2O$[9a] found to be isomorphous with zeolite ABW is denoted α-$LiZnPO_4 \cdot H_2O$ in the following. The polymorph of $LiZnPO_4 \cdot H_2O$ discovered in this study has similar unit cell parameters to those of α-$LiZnPO_4 \cdot H_2O$, but the *b* axis is doubled, therefore, denoted β-$LiZnPO_4 \cdot H_2O$. The synthesis, crystal structure and thermal properties of β-$LiZnPO_4 \cdot H_2O$ are now reported.

Experimental

Hydrothermal synthesis

In a search for new materials the system Li_2O–ZnO–P_2O_5–template was investigated by hydrothermal synthesis in aqueous and non-aqueous solutions using organic amine ions as templates. A synthesis was performed by dissolving $LiOH \cdot H_2O$ (3.677 g), LiCl (3.709 g) and $Zn(CH_3CO_2)_2 \cdot 2H_2O$ (18.971 g) in water (100 cm^3). Phosphoric acid, 85% H_3PO_4 (10.0 cm^3), and then ethyldiisopropylamine (30.0 cm^3) was slowly added with stirring giving a molar ratio of the reactants Li : Zn : PO_4 : $NEtPr^i_2$: water of 1.2 : 0.6 : 1 : 1.2 : ≈41, [PO_4] ≈ 0.9 M, pH 4.55

* E-Mail: trj@dou.dk

† *Non-SI unit employed*: bar = 101 325 Pa.

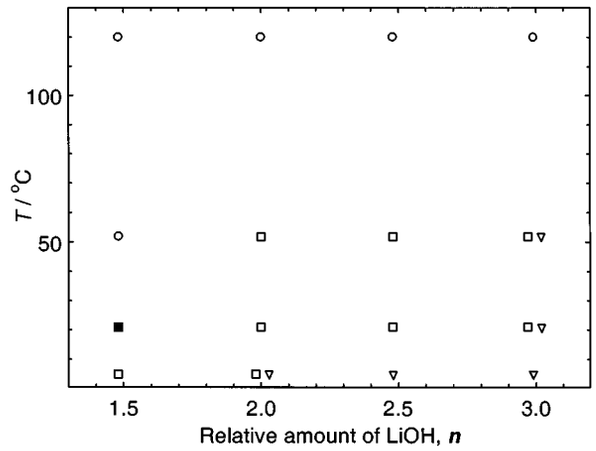

Fig. 1 The crystallisation fields of lithium zinc orthophosphates formed in the system LiOH–$Zn(CH_3CO_2)_2$–H_3PO_4–water, at varying amounts of LiOH, *n*, and temperature. In one case a phase-pure sample of β-$LiZnPO_4 \cdot H_2O$ (■) was obtained. Open symbols indicate impurities of β-Li_3PO_4, and α-$LiZnPO_4 \cdot H_2O$ is shown as triangles, β-$LiZnPO_4 \cdot H_2O$ as squares and α′-$LiZnPO_4$ as circles

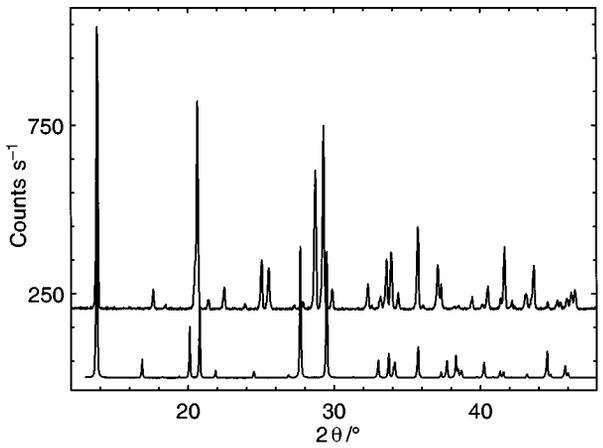

Fig. 2 Powder X-ray diffraction patterns of α- (bottom) and β-$LiZnPO_4 \cdot H_2O$

(measured 1 h after mixing). After stirring the gel for 1 h, powder diffraction showed the presence of α-$LiZnPO_4 \cdot H_2O$ of poor crystallinity along with a trace of an unidentified phase. A portion of the gel, *ca.* 5 cm^3, was left to stand for 3 months at room temperature, *ca.* 21 °C, before crystallisation was noticed and after 6 months the crystallisation was complete and the material (Sample **I**) was recovered by filtration and washed with deionised water. Another portion of the gel was heated at 55 °C for 3 months giving α-$LiZnPO_4 \cdot H_2O$ as product. The rest of the gel was heated to 200 °C for 68 h in a Teflon-lined steel autoclave giving δ_1-$LiZnPO_4$ as product.

In order to investigate the crystallisation fields of lithium zinc phosphates formed in the system LiOH–$Zn(CH_3CO_2)_2$–H_3PO_4–water, a number of syntheses were performed varying the amount of LiOH and the temperature. The LiOH and $Zn(CH_3CO_2)_2$ were dissolved in water and H_3PO_4 was slowly added with stirring forming a white gel. The relative amount of lithium is given as a variable *n*, relative to the amount of phosphoric acid: $n = n(Li)/n(PO_4)$. The molar composition of the synthesis mixtures, $Li : Zn : PO_4 : H_2O$, was $n : 0.52 : 1 : \approx 20$, where $n = 1.49$, 2.00, 2.48 or 2.99, $[PO_4] \approx 1.8$ M, $4.0 < pH < 7.2$, thermal treatment at 5, 21 or 52 °C for 28 d and at 120 °C for 6 d. The phase identification was performed by combining information from ^{31}P MAS NMR and powder diffraction and the products are displayed in Fig. 1. In one case a phase-pure sample of β-$LiZnPO_4 \cdot H_2O$ was obtained (filled square) and the other samples contained impurities of β-Li_3PO_4 (open symbols). At high temperatures, *e.g.* 120 °C, α′-$LiZnPO_4$ (circles) formed and at low temperatures α-$LiZnPO_4 \cdot H_2O$ (triangles) was found as product. Optimisation of the conditions for the hydrothermal synthesis revealed that templates were in fact not essential for the preparation of β-$LiZnPO_4 \cdot H_2O$. Several syntheses in the system LiOH–LiCl–$Zn(CH_3CO_2)_2$–H_3PO_4–$(CH_2OH)_2$ were performed in a similar way substituting the solvent water with ethylene glycol but gave only semiamorphous material with traces of α′-$LiZnPO_4$ and β-Li_3PO_4 as products.

A Teflon container holding a suspension of α-$LiZnPO_4 \cdot H_2O$ (0.381 g) in 0.9 M $LiNO_3$ (aq) (10 cm^3) and H_3PO_4 (0.1 cm^3) were heated in a PSIKA 20 kbar reactor at 80 °C and 10 kbar for 20 h, using oil as supporting fluid. The composition of the suspension was $Li : Zn : PO_4 : water = 2.6 : 0.58 : 1 : \approx 142$. The product was washed with ethanol (99.9%) and identified as β-$LiZnPO_4 \cdot H_2O$ using powder diffraction.

A Radiometer glass electrode combined with a calomel reference electrode (GK2401C) was used for pH measurements. The syntheses were performed using the following commercial chemicals: $LiOH \cdot H_2O$ (Fluka, puriss p.a., >99%), $LiNO_3$ (Merck, >98%), LiCl (Merck, pro analysi, >99%), H_3PO_4 (85%, Fluka, extra pure), $Zn(CH_3CO_2)_2 \cdot 2H_2O$ (Fluka, purum p.a. >99.0%), ethyldiisopropylamine (Aldrich, >99%) and ethylene glycol (Fluka, puriss p.a., >99.5%).

Powder diffraction

Powder diffraction data for phase identification and refinement of unit cell parameters were obtained using a Siemens D5000 diffractometer equipped with a primary germanium monochromator (Cu-$K\alpha_1$ radiation, $\lambda = 1.540\,598$ Å). The data were collected from 5 and up to 90° in 2θ with a step length of 0.02° and counting time of 2–15 s per step. The observed powder pattern of β-$LiZnPO_4 \cdot H_2O$ was distinctly different from that of the known zeolite type ABW polymorph, α-$LiZnPO_4 \cdot H_2O$, as shown in Fig. 2. The trial and error indexing program TREOR [14] revealed an orthorhombic unit cell of β-$LiZnPO_4 \cdot H_2O$ similar to the unit cell of α-$LiZnPO_4 \cdot H_2O$ with a doubled *b* axis. The program CELLKANT [15] was used to refine the unit cell parameters from the observed *d* spacings. The indexed powder pattern of β-$LiZnPO_4 \cdot H_2O$ (39 reflections, $I/I_0 > 2\%$) is given in Table 1 using the refined unit cell dimensions of β-$LiZnPO_4 \cdot H_2O$, $a = 10.030(1)$, $b = 16.553(2)$ and $c = 5.0120(5)$ Å, unit cell volume = 832.1(2) $Å^3$.

Single crystal diffraction

A clear, colourless octahedron of β-$LiZnPO_4 \cdot H_2O$ was selected from sample **I**. The data collection was performed on a Siemens SMART diffractometer equipped with a CCD detector and graphite monochromatised Mo-Kα radiation, $\lambda = 0.710\,73$ Å. Approximately one hemisphere of data was collected in frames covering 0.3° in ω in three sets at different φ angles using a detector to crystal distance of 40.0 mm. Data were corrected for Lorentz-polarisation effects and for absorption using Gaussian integration [transmission (maximum/minimum) 0.6383/0.3748] giving 1359 unique reflections.

A structural model was found using direct methods in space group $P2_1ab$, no. 29. This setting was chosen to resemble the unit cell of α-$LiZnPO_4 \cdot H_2O$ refined in space group $Pna2_1$, no. 33.[9a] Programs from the Siemens SHELXTL™ software package were used for structure solution and refinement.[16] After anisotropic refinement it was possible to locate the positions of the four hydrogen atoms in the Fourier-difference maps. The H atom positions and thermal parameters were not refined; all other atoms were refined with anisotropic thermal parameters. Scattering factors of neutral atoms were applied throughout. The refinement converged at $R = 0.0290$ and $R' = 0.0717$, with 146 parameters refined using full-matrix least squares based on all F^2. Atomic coordinates are shown in Table 2. Drawings of the crystal structure were prepared using the program ATOMS.[17]

Table 1 Indexed powder pattern of β-$LiZnPO_4 \cdot H_2O$

h	k	l	d_{calc}/Å	d_{obs}/Å	$(I/I_0)_{calc}$	$(I/I_0)_{obs}$
1	2	0	6.3838	6.3834	100	100
2	0	0	5.0152	5.0173	4	7
1	1	1	4.3275	4.3299	12	7
0	2	1	4.2872	4.2842	79	74
0	4	0	4.1382	4.1438	3	4
1	2	1	3.9422	3.9433	6	6
2	0	1	3.5452	3.5451	22	18
1	3	1	3.4796	3.4827	16	15
2	4	0	3.1919	3.1938	2	3
3	2	0	3.1001	3.1009	58	49
1	4	1	3.0409	3.0426	69	65
2	3	1	2.9826	2.9826	8	7
0	5	1	2.7623	2.7644	9	9
2	4	1	2.6923	2.6918	5	4
1	5	1	2.6632	2.6629	16	18
3	2	1	2.6365	2.6352	24	21
3	4	0	2.6007	2.6012	7	6
0	0	2	2.5060	2.5074	32	30
2	5	1	2.4196	2.4194	16	16
1	1	2	2.4055	2.4052	8	7
0	3	2	2.2817	2.2818	5	4
2	1	2	2.2214	2.2229	8	9
2	2	2	2.1645	2.1649	22	22
0	7	1	2.1386	2.1384	2	3
1	7	1	2.0916	2.0916	8	6
0	8	0	2.0691	2.0688	14	15
4	4	1	1.9717	1.9712	3	4
3	6	1	1.9587	1.9593	5	6
3	2	2	1.9489	1.9498	6	7
4	6	0	1.8562	1.8562	7	8
2	8	1	1.7870	1.7869	6	5
4	6	1	1.7402	1.7399	8	8
4	3	2	1.6876	1.6880	5	5
5	6	0	1.6225	1.6224	7	7
0	8	2	1.5955	1.5957	6	7
6	0	1	1.5858	1.5856	9	7
1	3	3	1.5790	1.5784	5	8
2	10	0	1.5719	1.5720	13	11
4	5	2	1.5627	1.5627	5	5

Crystal data. $LiO_4PZn \cdot H_2O$, $M = 185.30$, orthorhombic, space group $P2_1ab$ (no. 29), $a = 10.0224(9)$, $b = 16.5596(15)$, $c = 5.0126(5)$ Å, $U = 831.93(13)$ Å^3, $D_c = 2.959$, $D_m = 3.01$ g cm^{-3} (measured using a pycnometer and water), $T = 293$ K, $Z = 8$, μ(Mo-Kα) = 6.189 mm^{-1}, 3348 reflections measured, 1359 unique ($R_{int} = 0.0362$).

CCDC reference number 186/1004.

See http://www.rsc.org/suppdata/dt/1998/2261/ for crystallographic files in .cif format.

Spectroscopic investigation

Magic angle spinning ^{31}P NMR spectra were recorded on a Varian UNITY-500 spectrometer [11.7 T, $\nu(^{31}P) = 202.332$ MHz], using a Jakobsen MAS probe.[18] The samples were placed in a cylindrical rotor (Si_3N_4, 5 mm outside diameter, volume 220 μl). The free induction decays were recorded with a spinning speed of 5.5 kHz and the resulting spectra had a digital resolution of 2.5 Hz. An aqueous solution of H_3PO_4 (85%, Fluka, extra pure) was used as external standard. Infrared spectra were measured on a Perkin-Elmer 1720 Fourier-transform spectrometer using pellets of KBr containing 1% of the compound. The spectral resolution was 4 cm^{-1}.

Thermal investigation

A thermogravimetric (TG) measurement was performed between 30 and 500 °C, using a SETARAM TG 92-12 instrument, a nitrogen atmosphere and a heating rate of 5 °C min^{-1}. The sample was kept in an open Al_2O_3 crucible. Differential scanning calorimetry (DSC) was performed using a SETARAM DTA 92-16.18 instrument. The sample was placed in a platinum crucible and α-Al_2O_3 used as reference. The experiment was carried out between 20 and 900 °C using a heating and cooling rate of 5 °C min^{-1} in an argon atmosphere. Two experiments were carried out using the same sample. The temperature and enthalpy change calibration was carried out using the low–high quartz transition and the dehydration of $CaSO_4 \cdot 2H_2O$. Baseline fluctuations in the temperature range 20 to 130 °C are due to small differences between the set temperature and the actual temperature in the DSC instrument.

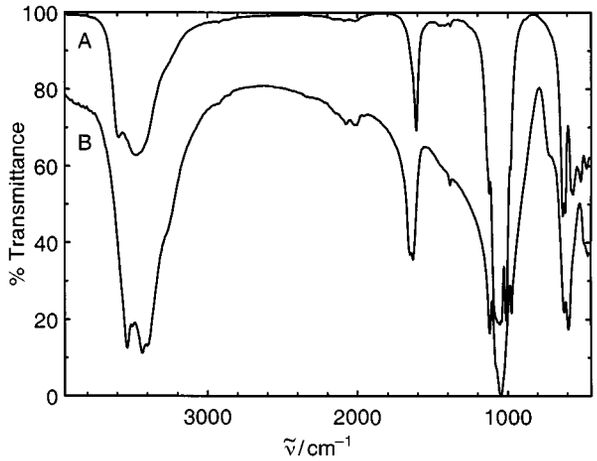

Fig. 3 Infrared spectra of α- (A) and β-$LiZnPO_4 \cdot H_2O$ (B)

Results and Discussion

Thermogravimetric measurements were in accordance with the formula β-$LiZnPO_4 \cdot H_2O$, observed weight loss 9.1% at 120–210 °C (calculated 9.7%). The density of β-$LiZnPO_4 \cdot H_2O$ was measured using pycnometry and water to $D_m = 3.01$ g cm^{-3}, and the calculated density was $D_c = 2.959$ g cm^{-3}. The density of α-$LiZnPO_4 \cdot H_2O$ is $D_c = 2.886$ g cm^{-3}.[9a]

Phosphorus-31 MAS NMR spectroscopy on β-$LiZnPO_4 \cdot H_2O$ showed two signals with chemical shifts δ(^{31}P) 6.94(2) and 7.88(2), in accordance with the crystallographic data revealing two phosphorus atoms in the asymmetric unit. The two polymorphs of $LiZnPO_4 \cdot H_2O$ thus have distinct phosphorus chemical shifts as α-$LiZnPO_4 \cdot H_2O$ shows only one signal [at δ(^{31}P) 6.05(2)].[9b]

Infrared spectra of the two polymorphs of $LiZnPO_4 \cdot H_2O$ are illustrated in Fig. 3. The absorptions at *ca.* 3500 and *ca.* 1600 cm^{-1} are due to stretch and bending vibrations in water molecules. A broad absorption in the spectrum of α-$LiZnPO_4 \cdot H_2O$ around 3400 cm^{-1} indicates the presence of adsorbed water, whereas multiple absorptions in the range 3300–3600 cm^{-1} suggest more than one inequivalent crystal water molecule in β-$LiZnPO_4 \cdot H_2O$. Orthophosphates generally show a strong absorption band in the range 940–1120 and medium at 540–650 cm^{-1}, due to framework vibrations.[19] Differences in this part of the spectra, Fig. 3, suggest differences in the framework structure of the two polymorphs, as will be discussed in the following.

Crystal structure of β-$LiZnPO_4 \cdot H_2O$

The crystal structure of β-$LiZnPO_4 \cdot H_2O$ is built from regular tetrahedra of ZnO_4 and PO_4 and slightly distorted tetrahedra of LiO_4. Selected bond lengths and angles are found in Table 3. Chains of alternating ZnO_4 and PO_4 tetrahedra run in the c direction. One half the chains have all tetrahedra pointing up (U) and the other chains have tetrahedra pointing down (D). Fig. 4(*a*) illustrates the connection between two chains forming zigzag four-ring chains parallel to the c axis. Fig. 4(*b*) displays how the double chains of four-ring chains are interconnected to

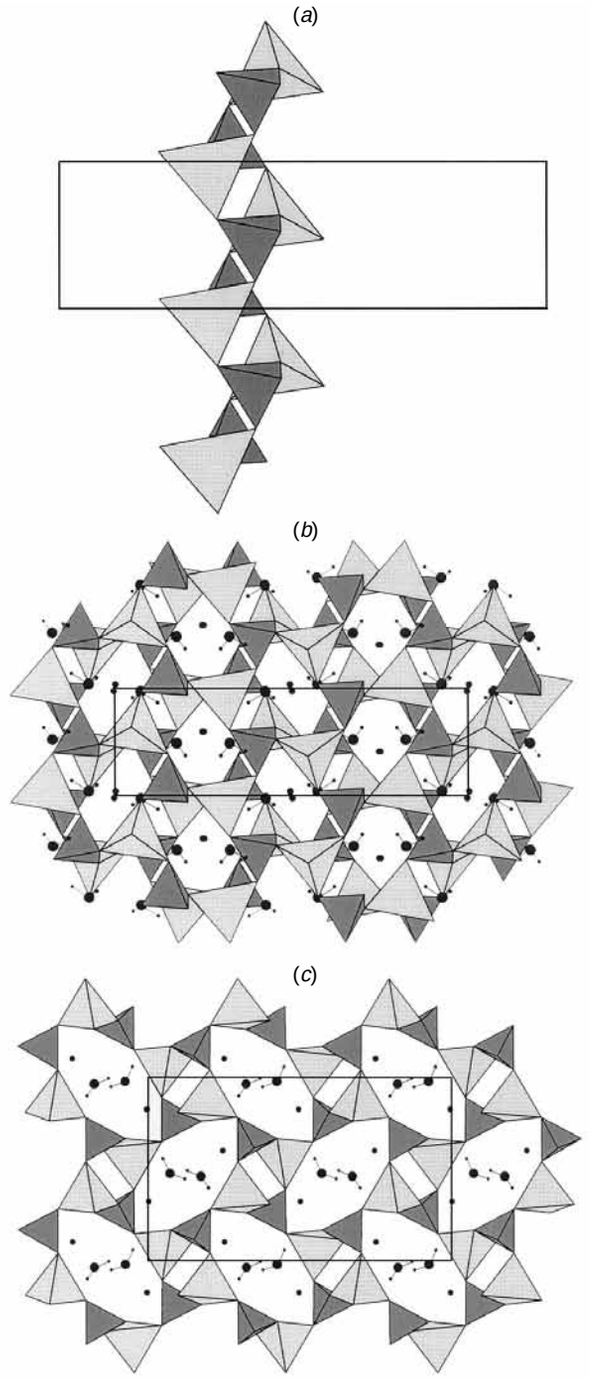

Fig. 4 Crystal structure of β-$LiZnPO_4 \cdot H_2O$: (*a*) the *b*,*c* projection, showing four-ring chains in the *c* direction; (*b*) connectivity of the four-ring chains forming nets of six-ring channels with stacking sequence, ABA, in the (100) direction; (*c*) the *a*,*b* projection, showing four- and eight-ring channels in the *c* direction with water and Li atoms placed in the eight rings. The ZnO_4 are grey and PO_4 are dark tetrahedra, lithium ions are shown as medium size black circles and water molecules as small (H atoms) and large (O atoms) black circles

form nets of six rings with the tetrahedra sequence UUUDDD, a characteristic feature of the ABW topology.[6b,13] Two types of six rings appear trigonally and ovally distorted having the symmetry of twofold axes and *a* glide planes, respectively. The trigonal shape resembles the shape of six rings found in the structures of α-$LiZnPO_4 \cdot H_2O$ and tridymite, whereas the oval resembles δ_I-$LiZnPO_4$ and cristobalite (the sequence of tetrahedra in a six ring of the three latter compounds are UDUDUD).[9b,20] The *b*,*c* projection, Fig. 4(*b*), consists of pseudo-hexagonal layers stacked with the sequence ABA to

Table 2 Atomic coordinates ($\times 10^4$) and equivalent isotropic displacement parameters ($Å^2 \times 10^3$) for β-$LiZnPO_4 \cdot H_2O$; U_{eq} is defined as one third of the trace of the orthogonalised U_{ij} tensor. Parameters for H atoms were not refined

Atom	*x*	*y*	*z*	U_{eq}
Zn(1)	1521(1)	6912(1)	4606(2)	10(1)
Zn(2)	9184(1)	5564(1)	1108(2)	10(1)
P(1)	8494(2)	6581(1)	5875(3)	7(1)
P(2)	7232(2)	4082(1)	149(4)	8(1)
Li(1)	9007(17)	7524(8)	923(20)	16(3)
Li(2)	1768(13)	4971(7)	4694(24)	15(3)
O(1)	9584(5)	7041(3)	4330(10)	13(1)
O(2)	1915(5)	5974(3)	6867(9)	13(1)
O(3)	2393(5)	6764(3)	1078(9)	11(1)
O(4)	8326(5)	5740(3)	4615(10)	10(1)
O(5)	1116(5)	5463(3)	1360(10)	12(1)
O(6)	8865(5)	6510(3)	8823(9)	12(1)
O(7)	2181(5)	7953(3)	5676(10)	14(1)
O(8)	8531(5)	4552(3)	9731(10)	12(1)
O(9)	393(6)	8247(3)	9846(11)	22(1)
O(10)	261(6)	4260(4)	5348(11)	23(1)
H(1)	1026	8000	8687	90
H(2)	84	8707	9102	90
H(3)	529	3788	6369	90
H(4)	9428	4500	5914	90

form a three-dimensional framework structure, as illustrated in Fig. 4(*c*) viewed along the *c* axis, showing another characteristic feature of the ABW topology: four- and eight-ring channels in the (001) direction. The water molecules and lithium ions are placed in the eight-ring channels as shown in Fig. 4(*c*).

Oxidation states, V_i, were calculated as a sum of bond valences, *s*, using the equation $s = \exp[(r_0 - r)/B]$, where r_0 and *B* are empirical parameters [r_0(P–O) = 1.617, r_0(Zn–O) = 1.704, r_0(Li–O) = 1.466, r_0(H–O) = 0.882 and *B* = 0.37 Å] and *r* is the bond length from the refined structural model.[21] The calculated oxidation states, V_i, are in Table 4, and the calculated values are in agreement with the expected oxidation states. The values of the oxygen atoms fall in three groups. The framework oxygen atoms co-ordinated to one P, Zn and Li each, O(1)–O(6), have calculated oxidation states, V_i, in the range 1.94–2.01. The framework oxygen atoms co-ordinated to two cations, O(7) and O(8), have lower V_i, 1.83 and 1.81, possibly due to a bond valence contribution from hydrogen bonding. The oxygen atoms in the water molecules, O(9) and O(10), gave values of 2.07 and 1.75, respectively. The low value of O(10) is due to long O(10)–H(3,4) bonds.

Comparison with related zeolite ABW type materials

A variety of different materials adopt the zeolite ABW type structure and crystallise with at least six different space group symmetries.[22] A new modification of the ABW structure is adopted by β-$LiZnPO_4 \cdot H_2O$ crystallising with space group symmetry $P2_1ab$. The material $LiAlSiO_4 \cdot H_2O$, zeolite Li-A(BW), and α-$LiZnPO_4 \cdot H_2O$ crystallise in the space group $Pna2_1$, *i.e.* the twofold screw axes are placed inside and parallel to the four-ring chains. The tetrahedra in each four ring are pairwise symmetry related and all tetrahedra point in the same direction viewed along the polar *c* axis in the structure of α- (see Fig. 5) whereas in β-$LiZnPO_4 \cdot H_2O$ one half point up and one half down, UUDD [see Fig. 4(*c*)]. In the structure of β-$LiZnPO_4 \cdot H_2O$ the twofold screw axes are in the centre of the six rings, and perpendicular to the four-ring chains, *i.e.* the tetrahedra in a four ring are crystallographically distinct.

The connectivity of the tetrahedra is the same for $LiAlSiO_4 \cdot H_2O$, α-$LiZnPO_4 \cdot H_2O$ and β-$LiZnPO_4 \cdot H_2O$; they all have the characteristic ABW topology and as other lithium-containing zeolitic materials they have high framework densities, 19.0, 18.8 and 19.2 T/1000 $Å^3$, respectively.

Table 3 Selected bond lengths (Å) and angles (°) for β-$LiZnPO_4 \cdot H_2O$. Symmetry transformations used to generate equivalent atoms: (*i*) $x-1, y, z$; (*ii*) $x, y, z-1$; (*iii*) $x+1, y, z$; (*iv*) $x+\frac{1}{2}, -y+\frac{3}{2}, z$; (*v*) $x+\frac{1}{2}, -y+1, -z+1$; (*vi*) $x+\frac{1}{2}, -y+1, -z$; (*vii*) $x+1, y, z-1$; (*viii*) $x-\frac{1}{2}, -y+1, -z+1$; (*ix*) $x-1, y, z+1$

Zn(1)–O(7)	1.922(5)	O(7)–Zn(1)–O(1^{i})	105.3(2)
Zn(1)–O(1^{i})	1.958(5)	O(7)–Zn(1)–O(2)	118.6(2)
Zn(1)–O(2)	1.964(5)	O(1^{i})–Zn(1)–O(2)	109.1(2)
Zn(1)–O(3)	1.988(5)	O(7)–Zn(1)–O(3)	102.0(2)
		O(1^{i})–Zn(1)–O(3)	112.7(2)
		O(2)–Zn(1)–O(3)	109.1(2)
Zn(2)–O(8^{ii})	1.927(5)	O(8^{ii})–Zn(2)–O(5^{iii})	106.7(2)
Zn(2)–O(5^{iii})	1.948(5)	O(8^{ii})–Zn(2)–O(6^{ii})	115.4(2)
Zn(2)–O(6^{ii})	1.967(5)	O(5)–Zn(2)–O(6^{ii})	105.5(2)
Zn(2)–O(4)	1.979(5)	O(8^{ii})–Zn(2)–O(4)	107.4(2)
		O(5^{iii})–Zn(2)–O(4)	112.8(2)
		O(6^{ii})–Zn(2)–O(4)	109.2(2)
P(1)–O(6)	1.528(5)	O(6)–P(1)–O(7^{iv})	108.1(3)
P(1)–O(7^{iv})	1.529(6)	O(6)–P(1)–O(4)	110.8(3)
P(1)–O(4)	1.538(5)	O(7^{iv})–P(1)–O(4)	109.6(3)
P(1)–O(1)	1.541(5)	O(6)–P(1)–O(1)	110.6(3)
		O(7^{iv})–P(1)–O(1)	109.1(3)
		O(4)–P(1)–O(1)	108.7(3)
P(2)–O(2^{v})	1.532(5)	O(2^{v})–P(2)–O(8^{ii})	109.9(3)
P(2)–O(8^{ii})	1.532(5)	O(2^{v})–P(2)–O(3^{vi})	111.0(3)
P(2)–O(3^{vi})	1.537(5)	O(8^{ii})–P(2)–O(3^{vi})	108.6(3)
P(2)–O(5^{vi})	1.546(5)	O(2^{v})–P(2)–O(5^{vi})	110.9(3)
		O(8^{ii})–P(2)–O(5^{vi})	107.5(3)
		O(3^{vi})–P(2)–O(5^{vi})	108.9(3)
Li(1)–O(9^{vii})	1.91(2)	O(9^{vii})–Li(1)–O(1)	106.6(8)
Li(1)–O(1)	1.972(12)	O(9^{vii})–Li(1)–O(6^{ii})	115.6(7)
Li(1)–O(6^{ii})	1.987(13)	O(1)–Li(1)–O(6^{ii})	97.9(6)
Li(1)–O(3^{iv})	2.00(2)	O(9^{vii})–Li(1)–O(3^{iv})	103.3(6)
		O(1)–Li(1)–O(3^{iv})	116.2(6)
		O(6^{ii})–Li(1)–O(3^{iv})	117.4(8)
Li(2)–O(10)	1.943(14)	O(10)–Li(2)–O(5)	97.8(6)
Li(2)–O(5)	1.971(13)	O(10)–Li(2)–O(2)	118.0(6)
Li(2)–O(2)	1.992(13)	O(5)–Li(2)–O(2)	98.2(6)
Li(2)–O(4^{viii})	1.985(13)	O(10)–Li(2)–O(4^{viii})	102.9(6)
		O(5)–Li(2)–O(4^{viii})	130.8(6)
		O(2)–Li(2)–O(4^{viii})	109.9(6)
O(9)–H(1)	0.952(5)	Li(1^{ix})–O(9)–H(1)	112.8(6)
O(9)–H(2)	0.904(6)	Li(1^{ix})–O(9)–H(2)	113.3(7)
O(10)–H(3)	0.972(6)	H(1)–O(9)–H(2)	109.8(5)
O(10)–H(4)	1.018(6)	Li(2)–O(10)–H(3)	111.2(6)
		Li(2)–O(10)–H(4)	84.3(6)
		H(3)–O(10)–H(4)	159.4(7)

Table 4 Calculated oxidation states, V_i, for the structure of β-$LiZnPO_4 \cdot H_2O$, using ref. 21

Cation	No.	V_i	Co-ordination number
Phosphorus	1	5.01	4
	2	4.97	4
Zinc	1	2.02	4
	2	2.03	4
Lithium	1	1.04	4
	2	1.02	4
Oxygen Framework	1	1.99	3
	2	2.00	3
	3	1.94	3
	4	1.96	3
	5	1.98	3
	6	2.01	3
	7	1.83	2
	8	1.81	2
Water	9	2.07	3
	10	1.75	3

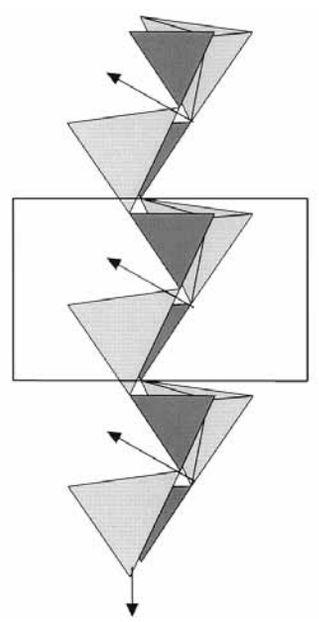

Fig. 5 Crystal structure of α-$LiZnPO_4 \cdot H_2O$, the *b*,*c* projection showing four-ring chains in the *c* direction. The arrows indicate a mechanism for a displacive phase transition of α- to β-$LiZnPO_4 \cdot H_2O$, *i.e.* the tetrahedra in the lower chain are rotated by *ca.* 45° and the upper chain is moved slightly downwards. The ZnO_4 are shown as grey and PO_4 as dark tetrahedra

Synthesis

In a previous study α-$LiZnPO_4 \cdot H_2O$ was found to crystallise from the system $LiOH–Zn(NO_3)_2–H_3PO_4$–water.[4] Hydrothermal syntheses from the system $LiOH–Zn(CH_3CO_2)_2–H_3PO_4$–water suggest that α-$LiZnPO_4 \cdot H_2O$ is in fact a metastable intermediate phase that transforms to β-$LiZnPO_4 \cdot H_2O$, *i.e.* the system approaches higher density and higher thermodynamic stability: gel ⟶ α-$LiZnPO_4 \cdot H_2O$ ⟶ β-$LiZnPO_4 \cdot H_2O$. The material α-$LiZnPO_4 \cdot H_2O$ has only been obtained as a microcrystalline powder, whereas β-$LiZnPO_4 \cdot H_2O$ can be obtained as larger crystals. This is probably due to the very different timescales of nucleation and crystal growth for α- and β-$LiZnPO_4 \cdot H_2O$.

Thermal investigation

Phase transformations of α- and β-$LiZnPO_4 \cdot H_2O$ were investigated by hydrothermal and dry heating. Hydrothermal heating of α-$LiZnPO_4 \cdot H_2O$ at ultra high pressure (80 °C, 10 kbar, 20 h) produced β-$LiZnPO_4 \cdot H_2O$, *i.e.* approaching higher density. Fig. 5 shows the *b*,*c* projection of α-$LiZnPO_4 \cdot H_2O$ with four-ring chains in the *c* direction and arrows indicate how α- transforms into β-$LiZnPO_4 \cdot H_2O$ by a displacive phase transition [compare Fig. 5 and 4(*a*)]. Half the chains of tetrahedra (the lower chain in Fig. 5) are distorted as indicated by the arrows, *i.e.* the tetrahedra are rotated by *ca.* 45°. The tetrahedra in the upper chain are all moved slightly. The mean angle between the framework tetrahedral atoms, T–O–T angles, in α- and β-$LiZnPO_4 \cdot H_2O$ are similar, 125.2 and 128.3°, respectively.

Hydrothermal heating of α-$LiZnPO_4 \cdot H_2O$ at $T > 100$ °C was found to produce δ_I-$LiZnPO_4$,[9] and the mechanism appeared to be solution mediated.[23] The compound β-$LiZnPO_4 \cdot H_2O$ also transforms into δ_I-$LiZnPO_4$ upon hydrothermal treatment at >100 °C. The dry heating dehydration of β-$LiZnPO_4 \cdot H_2O$ was investigated using differential scanning calorimetry giving an enthalpy change of $\Delta H = 43(6)$ kJ mol^{-1}, peak value at 219(2) °C, for the irreversible phase transformation of β-LiZn-

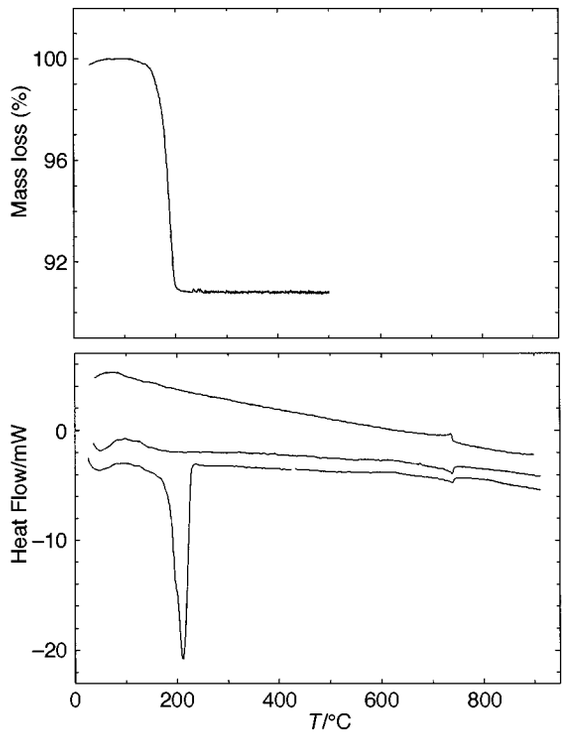

Fig. 6 Thermal investigation of β-$LiZnPO_4 \cdot H_2O$ showing the mass loss detected by thermogravimetry (upper graph) and differential scanning calorimetry; the lower and the middle DSC curves are the first and second heating and the upper DSC curve is one of the very similar cooling curves

$PO_4 \cdot H_2O$ into δ_I-$LiZnPO_4$. A shoulder, at *ca.* 206 °C, was found on the DSC signal for the dehydration, Fig. 6, but the TG trace suggests a one-step process. A weak signal at 738(1) °C shows the phase transition of δ_I-$LiZnPO_4$ into β-$LiZnPO_4$ in accordance with the equilibrium phase diagram.[11] The DSC trace resembles a shift in baseline indicating that mainly a change in heat capacity is taking place. Cooling β-$LiZnPO_4$ produces α-$LiZnPO_4$ [$a = 17.240(2)$, $b = 9.768(1)$, $c = 17.106(1)$ Å and $\beta = 110.90(1)°$, refined from powder diffraction data, 118 reflections] and the α- to β-$LiZnPO_4$ phase transition is shown to be reversible in Fig. 6.

The zeolites $MAlSiO_4 \cdot xH_2O$ (M = Li, Na or Ag) show a large framework flexibility as the dehydrated polymorphs may retain the ABW topology and the aluminosilicates of Na and Ag have partly dehydrated ABW polymorphs ($x = 0.8$ and $x = 0.8$ and 0.68, respectively).[24] Further heating of the dehydrated ABW type $LiAlSiO_4$ produces a stuffed cristobalite-type structure,[24b] which is similar to the phase transition of α- and β-$LiZnPO_4 \cdot H_2O$ to δ_I-$LiZnPO_4$.

Conclusion

Investigation of the system $LiOH–Zn(CH_3CO_2)_2–H_3PO_4$–water, revealed that a new phase of $LiZnPO_4 \cdot H_2O$ can be prepared under ambient conditions. A known polymorph of $LiZnPO_4 \cdot H_2O$ (ABW structure, space group $Pna2_1$) was found as an intermediate phase during the synthesis and transforms into β-$LiZnPO_4 \cdot H_2O$ by hydrothermal heating at ultra high pressure. A mechanism for the displacive phase transition is proposed. Hydrothermal or dry heating of β-$LiZnPO_4 \cdot H_2O$ at >100 °C produces δ_I-$LiZnPO_4$. The crystal structure of β-$LiZnPO_4 \cdot H_2O$ can be viewed as framework structures built from PO_4 and ZnO_4 tetrahedra with LiO_4 tetrahedra and water molecules placed in eight-ring channels running in the *c* direction. This compound is apparently the only member of the zeolite ABW group of materials crystallising in space group $P2_1ab$.

Acknowledgements

R. G. Hazell, P. Norby (Aarhus University), P. C. Stein, O. Simonsen and E. M. Skou (Odense University) are thanked for valuable discussions. A Danish Technical Research Council Ph.D. grant is gratefully acknowledged. The Siemens SMART diffractometer at the Chemistry Department, Aarhus University was partly financed by Carlsberg fondet. I am grateful to M. B. Nielsen for help. The PSIKA 20 kbar reactor at the Chemistry Department, Odense University was financed by The Danish Natural Science Research Council.

References

1 C. P. Grey, F. I. Poshni, A. F. Gualtieri, P. Norby, J. C. Hanson and D. R. Corbin, *J. Am. Chem. Soc.*, 1997, **119**, 1981; Yun-Jo Lee and Hakze Chon, *J. Chem. Soc., Faraday Trans.*, 1996, 3453; H. van Bekkum, E. M. Flanigen and J. C. Jansen, *Stud. Surf. Sci. Catal.*, 1991, **58**.
2 (*a*) M. Estermann, L. B. McCusker, C. Baerlocher, A. Merrouche and H. Kessler, *Nature* (*London*), 1991, **352**, 320; (*b*) V. Soghomonian, Qin Chen, R. C. Haushalter, J. Zubieta and C. J. O'Connor, *Science*, 1993, **259**, 1596; (*c*) G. W. Noble, P. A. Wright and Å. Kvick, *J. Chem. Soc., Dalton Trans.,* 1997, 4485; (*d*) Pingyun Feng, Xianhui Bu and G. D. Stucky, *Nature* (*London*), 1997, **388**, 735; (*e*) Sue-Lein Wang, Kuei-Fang Hsu and Yeu-Perng Nieh, *J. Chem. Soc., Dalton Trans.*, 1994, 1681; (*f*) Pingyun Feng, Xianhui Bu and G. D. Stucky, *Acta Crystallogr., Sect. C*, 1997, **53**, 997; (*g*) T. R. Jensen, P. Norby, J. C. Hanson, E. M. Skou and P. C. Stein, *J. Chem. Soc., Dalton Trans.*, 1998, 527.
3 Tianyou Song, M. B. Hursthouse, Jiesheng Chen, Jianing Xu, K. M. A. Malik, R. H. Jones, Ruren Xu and J. M. Thomas, *Adv. Mater.*, 1994, **6**, 679; ref. 2(*g*) and refs. therein.
4 T. E. Gier and G. D. Stucky, *Nature* (*London*), 1991, **349**, 508.
5 Tianyou Song, Jianing Xu, Yu-e Zhao, Yong Yue, Yihua Xu, Ruren Xu, Ninghai Hu, Gecheng Wei and Hengqing Jia, *J. Chem. Soc., Chem. Commun.*, 1994, 1171.
6 (*a*) W. T. A Harrison and L. Hannooman, *Angew Chem., Int. Ed. Engl.*, 1997, **36**, 640; (*b*) W. M. Meier and D. H. Olsen, *Atlas of Zeolite Structure Types*, 3rd edn., Butterworth-Heinemann, London, 1992.
7 T. R. Jensen, unpublished work.
8 Xianhui Bu, T. E. Gier and G. D. Stucky, *Acta Crystallogr., Sect. C*, 1996, **52**, 1601.
9 (*a*) W. T. A. Harrison, T. E. Gier, J. M. Nicol and G. D. Stucky, *J. Solid State Chem.*, 1995, **114**, 249; (*b*) T. R. Jensen, P. Norby, P. C. Stein and A. M. T. Bell, *J. Solid State Chem.*, 1995, **117**, 39.
10 J. A. Gard, G. Torres-Trevino and A. R. West, *J. Mater. Sci. Lett.*, 1985, **4**, 1138; L. Elammari and B. Elouadi, *Acta Crystallogr., Sect. C*, 1989, **45**, 1864.
11 G. Torres-Trevino and A. R. West, *J. Solid State Chem.*, 1986, **61**, 56.
12 T. R. Jensen and A. Nørlund Christensen, unpublished work.
13 P. Norby, A. Nørlund Christensen and I. G. Krogh Andersen, *Acta Chem. Scand., Sect. A*, 1986, **40**, 500; E. Krogh Andersen and G. Ploug-Sørensen, *Z. Kristallogr.*, 1986, **176**, 67.
14 P.-E. Werner, L. Eriksson and M. Westdahl, *J. Appl. Crystallogr.*, 1985, **18**, 367.
15 N. O. Ersson, CELLKANT, Chemical Institute, Uppsala University, Uppsala, 1981.
16 G. M. Sheldrick, SHELXTL, Siemens Analytical X-Ray Systems Inc., Madison, WI, 1995.
17 E. Dowty, ATOMS, version 4.0, Shape Software, Kingsport, TN, 1997.
18 H. J. Jakobsen, P. Daugaard and V. Langer, *J. Magn. Reson.*, 1988, **76**, 162; *U.S. Pat.*, 4 739 270, 1988.
19 R. A. Nyquist and R. O. Kagel, *Infrared spectra of inorganic compounds*, Academic Press, New York and London, 1971, p. 11.
20 A. Putnis, *Introduction to mineral sciences*, Cambridge University Press, 1992, p. 172.
21 I. D. Brown and D. Altermatt, *Acta Crystallogr., Sect. B*, 1985, **41**, 244.
22 P. Norby, Ph.D. Thesis, University of Aarhus, 1989.
23 T. R. Jensen, P. Norby and J. C. Hanson, unpublished work.
24 (*a*) P. Norby and H. Fjellvåg, *Zeolites*, 1992, **12**, 898; (*b*) P. Norby, *Zeolites*, 1990, **10**, 193.

Received 17*th March* 1998; *Paper* 8/02113I